incidences of bronchiolo-alveolar adenomas/carcinomas in the lung by Peto's test. In the same test, significant positive trends were shown for hepatocellular adenomas and combined incidences of hepatocelluar adenomas/carcinomas. The incidence of bronchiolo-alveolar adenomas in the 3200 ppm-exposed group exceeded the maximum tumor incidence in the historical control data. In addition, the combined incidence of bronchiolo-alveolar adenomas/carcinomas was significantly increased in the 3200 ppm-exposed group by Fisher's exact test, and the incidence exceeded the respective maximum tumor incidence in the historical control data. Hepatocellular adenomas were significantly increased in the 200, 800 and 3200 ppm-exposed groups by Fisher's exact test, and the incidences exceeded the respective maximum tumor incidence in the historical control data. The combined incidence of hepatocellular adenomas/carcinomas significantly increased in the 800 and 3200 ppm-exposed mice, and the tumor incidences in the 200, 800 and 3200 ppm-exposed groups exceeded the respective maximum tumor incidences of the historical control data. The hepatocellular adenomas were well-circumscribed lesions compressing adjacent parenchyma and lacking normal lobular architecture, composed of well-differentiated hepatocytes (Figure 3D). Exposure-related, neoplastic lesions other than those listed in Table 3 were not observed in female mice. No exposure-related non-neoplastic lesions occurred in any of the TCE-exposed groups.

Discussion

This study demonstrated that 2-year inhalation exposure to TCE vapor significantly increased incidences of benign and malignant tumors in several organs of rats and mice.

In male rats, bronchiolo-alveolar adenomas in the lung and abdominal peritoneal mesotheliomas were induced by the 2-year exposure to TCE on the basis of the following evidence. Incidences of these tumors were increased in a concentration-dependent manner, with a significant positive trend. The increase in bronchiolo-alveolar adenomas at the 800 ppm group and peritoneal mesotheliomas at the 3200 ppm group attained statistical significance by Fisher's exact test. Additionally, the incidences of those tumors in the 3200 ppm-exposed group, as well as the incidence of bronchiolo-alveolar adenomas in the 800 ppm-exposed group, exceeded the respective maximum tumor incidences in the JBRC historical control data.

In male mice, concentration-dependent increase in the incidences of malignant lymphomas of spleen and Harderian gland adenomas were evidenced by significant positive trends. The increase in Harderian gland tumors in the 3200 ppm group attained statistical significance by Fisher's exact test. In addition, the incidences of tumors (spleen and Harderian gland) in the 3200 ppm-exposed group exceeded the maximum tumor incidence in the historical control data.

In female mice, concentration-dependent increase in the incidences of bronchiolo-alveolar adenomas, bronchiolo-alveolar adenomas/carcinomas combined, hepatocellular adenomas and hepatocellular adenomas/carcinomas combined were evidenced by significant positive trends. The incidences of pulmonary tumors in the 3200 ppm-exposed group exceeded the maximum tumor incidence in the historical control data. The increases of combined incidence of hepatocellurar adenomas/carcinomas in the 800 and 3200 ppm-exposed groups attained statistical significance by Fisher's exact test. Furthermore, the incidences of hepatic tumors in the 200, 800 and 3200 ppm-exposed groups exceeded the maximum incidence in the historical control data.

In the study of Quast et al. (1988), male and female of Fischer 344 rats and B6C3F1 mice were exposed to 0, 150, 500 or 1500 ppm TCE vapor for 6 h/d, 5 d/week for 2 years. Inhalation exposure of Fischer 344 rats to 1500 ppm TCE vapor resulted in a slight reduction of the body weights in females. While very slight microscopic hepatic effects were seen in the livers of 1500 ppm-exposed male and female rats necropsied at 6, 12 and 18 months (using 10 rats), hepatic tumors were not observed at 24 months (using 50 rats). There were no toxic effects noted in mice at any exposure concentrations of TCE. Particularly, there were no indications of oncogenic effects in rats or mice following the 2-year exposure of TCE. However, it was noted in the IRIS report (U.S. EPA, 2007) that the exposure levels were too low, because the MTD was not reached in mice (no adverse effects observed in either sex) and may not have been reached in rats.

In the present carcinogenicity study of rats and mice, selection of the highest concentration, 3200 ppm was appropriate for evaluating carcinogenic potency of TCE for the following reasons. First, terminal body weights of TCE-exposed rats and mice were less than 10% as compared with those of respective controls. Second, there was no significant difference in the survival rate between any of the TCE-exposed rat and mouse groups and the respective controls except for the survival rate of 3200 ppm-exposed male mice. The present data for both 2-year survival rates and the terminal body weight decrease without any overt manifestation of chronic non-neoplastic lesions in the TCE-exposed animals can be taken to fulfill the MTD criteria, indicating that the highest concentrations of 3200 ppm did not exceed the MTD in accordance with the prediction from the 13-week inhalation exposure study.

In this study, the tumors which significantly increased in the female mice exposed to 200 and 800 ppm TCE were hepatocellurar adenomas. Quast et al. (1988) reported that mice exposed to TCE at the highest dose of 1500 ppm did not have tumors in the 2-year study. This study used the Crj: BDF1 mice, whereas Quast used the B6C3F1 mice. Therefore, strain differences may contribute to sensitivity of TCE hepatocarcinogenicity.

The results of mutagenicity studies for TCE with *Salmonella typhimurium* TA100 and TA1535 in the presence and absence of metabolic activation were positive with vapor phase (JETOC, 2005a). The results of chromosome aberrations in cultured Chinese hamster ovary cells were also positive (Galloway et al., 1987). In addition, the results of cell transformation assays were positive (Hatch et al., 1983). Therefore, it is possible that a genotoxic mode of action operates in TCE -induced carcinogenesis.

For the metabolism of TCE, Schumann et al. (1982) reported studies on the pharmacokinetics of [^{14}C] TCE in male Fischer 344 rats and B6C3F1 mice undertaken to

RIGHTSLINK

characterize the disposition of the inhaled chemical over a wide range of exposure concentrations. The major elimination route of TCE was via exhalation of unchanged chemical in expired air, accounting approximately 94%–98% of the total recovered radioactivity in rats and 87%–97% in mice at 150 and 1500 ppm, respectively. In addition, Nolan et al. (1984) reported that over 91% of the absorbed TCE was excreted unchanged.

Mesotheliomas are tumors that arise from the serosal surface of the pleura, peritoneum and pericardium. They also originate from the oil-rich tunica vaginalis of the testis manifested as a paratesticular mass (Brimo et al., 2010). The octanol–water partition coefficient (TCE: 2.49) of TCE is higher than the octanol–water partition coefficient (1,2-dichloroethane (DCE): 1.48, dichloromethane (DCM): 1.3) (WHO, 2003a,b,c). Hence, it would be expected that the high lipid soluble TCE was concentrated on the serosal surface of the peritoneum, where it induced mesotheliomas.

The highly significant incidences of peritoneal methotheliomas in male rats and hepatocellular adenomas in the female mice clearly indicate that they were caused by TCE-inhalation exposure. Of note, the incidences of these neoplastic lesions are higher than those in the carcinogenicity study in the rats and mice for inhalation exposure of TCE-related compounds, DCE (Nagano et al., 2006) and DCM (Aiso et al., 2001), carried out by JBRC. Moreover, hepatocellular adenomas were also induced by the administration of DCE and DCM in the female mice, and the sex dependence may be related to the fact that sex differences exist in the reported evidence of DNA adducts and mutagenesis (JETOC, 2005a,b,c). In addition, NTP reported that oral administration of 1,2,3-trichloropropane, a related substance of TCE, resulted in the development of neoplasms of the liver and Harderian gland in male and female mice (NTP, 1993).

In conclusion, the present study provided clear evidence of carcinogenicity for TCE on inhalation exposure in rats and mice.

Acknowledgements

The author thank Ms. Haruka Tomono (Sophia University) for detailed review of this manuscript. We also acknowledge the technical support of Mr Masahiro Yamamoto, Mr Yasutomo Sasaki and Mrs. Mieko Saito.

Declaration of interest

The present studies were contracted and supported by the Ministry of Health, Labour and Welfare of Japan. The authors declare that there are no conflicts of interest.

References

Aiso S, Saito A, Ohsawa M, et al. (2001). Carcinogenesis studies of dichloromethane in F344 rats and BDF1 mice (inhalation study). Proceeding of The Japanese Cancer Association, 60th Annual Meeting. Jpn J Cancer Res 92:277.

American Conference on Governmental Industrial Hygienists (ACGIH). (2001). 1,1,1-Trichloroethane. Documentation of the threshold limit values (TLVs) and biological exposure indices (BEIs) [CD-ROM]. Cincinnati, OH: ACGIH.

Brimo F, Illei PB, Epstein JI. (2010). Mesothelioma of the tunica vaginalis: a series of eight cases with uncertain malignant potential. Mod Pathol 23:1165–72.

Galloway SM, Armstrong MJ, Reuben C, et al. (1987). Chromosome aberrations and sister chromatid exchanges in Chinese hamster ovary cells: evaluations of 108 chemicals. Environ Mol Mutagen 10:1 175.

Hatch GG, Mamay PD, Ayer ML, et al. (1983). Chemical enhancement of viral transformation in Syrian hamster embryo cells by gaseous and volatile chlorinated methanes and ethanes. Cancer Res 43: 1945–50.

International Agency for Research on Cancer (IARC). (1999). 1,1,1-Trichloroethane. Re-evaluation of some organic chemicals, hydrazine and hydrogen peroxide (Part Two). IARC Monogr Eval Carcinogen Risk Hum 71:881–903.

Japan Chemical Industry Ecology-Toxicology & Information Center (JETOC). (2005a). Mutagenicity in bacterial test data of existing chemical substances: based on toxicity investigation system of the Industrial Safety and Health Law (1,1,1-trichloroethane). Tokyo: JETOC, B0105.

Japan Chemical Industry Ecology-Toxicology & Information Center (JETOC). (2005b). Mutagenicity in bacterial test data of existing chemical substances: based on toxicity investigation system of the Industrial Safety and Health Law (1,2 dichloroethane). Tokyo: JETOC, B0009.

Japan Chemical Industry Ecology-Toxicology & Information Center (JETOC). (2005c). Mutagenicity in bacterial test data of existing chemical substances: based on toxicity investigation system of the Industrial Safety and Health Law (dichloromethane). Tokyo: JETOC, B9414.

Japan Society for Occupational Health (JSOH). (2010). Recommendation of occupational exposure limits 1974. J Occup Health 52:313.

Japanese Association for Laboratory Animal Science (JALAS). (1987). Guideline for animal experimentation. Exp Anim 36:285–8.

Kaplan EL, Meier P. (1958). Nonparametric estimation from incomplete observations. Am Stat Assoc J 53:457–81.

Montzka SA, Butler JH, Elkins JW, et al. (1999). Present and future trends in the atmospheric burden of ozone-depleting halogens. Nature 398:690–4.

Montzka SA, Butler JH, Myers RC, et al. (1996). Decline in the tropospheric abundance of halogen from halocarbons: implications for stratospheric ozone depletion. Science 272:1318–22.

Nagano K, Umeda Y, Senoh H, et al. (2006). Carcinogenicity and chronic toxicity in rats and mice exposed by inhalation to 1,2-dichloroethane for two years. J Occup Health 48:424–36.

National Toxicology Program (NTP). (1993). Toxicology and carcinogenesis studies of 1,2,3,-trichloropropane in F344/N rats and B6C3F1 mice (gavage studies). NTP Technical Report Series No. 384. Bethesda: NTP.

Nolan RJ, Freshour NL, Rick DL, et al. (1984). Kinetics and metabolism of inhaled methyl chloroform (1,1,1-trichloroethane) in male volunteers. Fundam Appl Toxicol 4:654–62.

Organization for Economic Cooperation and Development. (1981a). OECD guideline for testing of chemicals 453 "combined chronic toxicity/carcinogenicity studies". Adopted May 1981. Paris: OECD.

Organization for Economic Cooperation and Development. (1981b). OECD principles of good laboratory practice. Adopted 1981. Paris: OECD.

Peto R, Pike MC, Armitage P, et al. (1977). Design and analysis of randomized clinical trials requiring prolonged observation of each patient. II. Analysis and examples. Br J Cancer 35:1–39.

Peto R, Pike MC, Day NE, et al. (1980). Guidelines for simple, sensitive significance tests for carcinogenic effects in long-term animal experiments. IARC Monogr Eval Carcinog Risk Chem Hum Suppl 2:311–426.

Quast JF, Calhoun LL, Frauson LE. (1988). 1,1,1-Trichloroethane formulation: a chronic inhalation toxicity and oncogenicity study in Fischer 344 rats and B6C3F1 mice. Fundam Appl Toxicol 11: 611–25.

Reimann S, Manning AJ, Simmonds PG, et al. (2005). Low European methyl chloroform emissions inferred from long-term atmospheric measurements. Nature 433:506–8.

Schumann AM, Fox TR, Watanabe PG. (1982). [^{14}C]Methyl chloroform (1,1,1 trichloroethane): pharmacokinetics in rats and mice following inhalation exposure. Toxicol Appl Pharmacol 62:390–401.

United Nations Environment Programme (UNEP). (2003). The 1987 Montreal Protocol on Substances that Deplete the Ozone Layer as adjusted and amended by the second, fourth and seventh meetings

RIGHTSLINK

of the parties. In: Handbook for the International Treaties for the Protection of the Ozone Layer. 4th ed. Nairobi, Kenya: UNEP, 18–39.

U.S. Environmental Protection Agency (EPA). (2007). 1,1,1-Trichloroethane. Integrated Risk Information System (IRIS). EPA. Available from: http://www.epa.gov/iris/toxreviews/0197tr.pdf [last accessed 21 Sept 2012].

WHO. (2003a). 1,1,1-Trichloroethane in drinking-water. Background document for development of WHO Guidelines for Drinking water Quality. WHO/SDE/WSH/03.04.65 [Online]. Available from: http://www.who.int/water sanitation health/dwq/chemicals/111-Trichloroethane.pdf [last accessed 21 Sept 2012].

WHO. (2003b). 1.2 Dichloromethane in drinking water. Background document for development of WHO guidelines for drinking-water quality. WHO/SDE/WSH/03.04.67 [Online]. Available from: http://www.who.int/water sanitation health/dwq/chemicals/12-Dichloroethane.pdf [last accessed 21 Sept 2012].

WHO. (2003c). Dichloroethane in drinking water. Background document for development of WHO guidelines for drinking-water quality. World Health Organization [Online]. Available from: http://www.who.int/water_sanitation_health/dwq/chemicals/dichloromethane.pdf [last accessed 21 Sept 2012].

World Meteorological Organization (WMO). (2012). WMO WDCGG data summary. Japan Meteorological Agency, World Meteorological Organization [Online]. Available from: http://ds.data.jma.go.jp/gmd/wdcgg/products/summary/sum36/sum36.pdf [last accessed 21 Sept 2012].

RIGHTSLINK

The Journal of Toxicological Sciences (J. Toxicol. Sci.)
Vol.37, No.2, 373-380, 2012

Original Article

Development of humanized steroid and xenobiotic receptor mouse by homologous knock-in of the human steroid and xenobiotic receptor ligand binding domain sequence

Katsuhide Igarashi[1], Satoshi Kitajima[1], Ken-ichi Aisaki[1], Kentaro Tanemura[1], Yuhji Taquahashi[1], Noriko Moriyama[1], Eriko Ikeno[1], Nae Matsuda[1], Yumiko Saga[2,3], Bruce Blumberg[4] and Jun Kanno[1]

[1]Division of Cellular and Molecular Toxicology, Biological Safety Research Center, National Institute of Health Sciences, 1-18-1 Kamiyoga, Setagaya-ku, Tokyo, 158-8501, Japan
[2]Division of Mammalian Development, National Institute of Genetics, Yata 1111, Mishima 411-8540, Japan
[3]The Graduate University for Advanced Studies (Sokendai), Yata 1111, Mishima 411-8540, Japan
[4]Department of Developmental and Cell Biology, 2011 Biological Sciences 3, University of California, Irvine, CA 92697-2300, USA

(Received December 7, 2011; Accepted January 12, 2012)

ABSTRACT — The human steroid and xenobiotic receptor (SXR), (also known as pregnane X receptor PXR, and NR1I2) is a low affinity sensor that responds to a variety of endobiotic, nutritional and xenobiotic ligands. SXR activates transcription of Cytochrome P450, family 3, subfamily A (CYP3A) and other important metabolic enzymes to up-regulate catabolic pathways mediating xenobiotic elimination. One key feature that demarcates SXR from other nuclear receptors is that the human and rodent orthologues exhibit different ligand preference for a subset of toxicologically important chemicals. This difference leads to a profound problem for rodent studies to predict toxicity in humans. The objective of this study is to generate a new humanized mouse line, which responds systemically to human-specific ligands in order to better predict systemic toxicity in humans. For this purpose, the ligand binding domain (LBD) of the human SXR was homologously knocked-in to the murine gene replacing the endogenous LBD. The LBD-humanized chimeric gene was expressed in all ten organs examined, including liver, small intestine, stomach, kidney and lung in a pattern similar to the endogenous gene expressed in the wild-type (WT) mouse. Quantitative reverse transcription-polymerase chain reaction (RT-PCR) analysis showed that the human-selective ligand, rifampicin induced Cyp3a11 and Carboxylesterase 6 (Ces6) mRNA expression in liver and intestine, whereas the murine-selective ligand, pregnenolone-16-carbonitrile did not. This new humanized mouse line should provide a useful tool for assessing whole body toxicity, whether acute, chronic or developmental, induced by human selective ligands themselves and subsequently generated metabolites that can trigger further toxic responses mediated secondarily by other receptors distributed body-wide.

Key words: Steroid and xenobiotic receptor, Pregnane X receptor, Humanized mouse, Ligand binding domain, Knock-in mouse

INTRODUCTION

Most orally administered xenobiotics are metabolized first by the intestine and then by the liver after portal transport. The expression levels of enzymes involved in xenobiotic metabolism are regulated at the transcriptional level by key xenobiotic sensors including the steroid and xenobiotic receptor (SXR), also known as the pregnane X receptor (PXR), pregnane activated receptor (PAR) and NR1I2 (Bertilsson *et al.*, 1998; Lehmann *et al.*, 1998; Blumberg *et al.*, 1998). SXR is important in the field of toxicology for at least two reasons. Firstly, this receptor system induces the expression of CYP3A and CYP2B enzymes, the major metabolizers of pharmaceu-

Correspondence: Jun Kanno (E-mail: kanno@nihs.go.jp)

ticals and xenobiotics. Therefore, SXR is a key mediator of drug- and chemical-induced toxicity as well as drug-drug and drug-nutrient interactions (Zhou *et al.*, 2004). Secondly, the orthologous rodent and human receptors exhibit differential sensitivity for a subset of chemical ligands important in the field of toxicology. For example, rifampicin (RIF) is a specific and selective activator of human SXR, whereas pregnenolone 16a-carbonitrile (PCN) is selective for the rodent orthologue.

Rodent-human differences in CYP3A and CYP2B-mediated responses to xenobiotics can be a profound problem in toxicologic studies where rodents are used to predict the toxicity of a compound in humans (Ma *et al.*, 2007). Therefore, development of a murine model that reconstructs the SXR-mediated systemic response of humans is of a great significance in toxicology.

Human and rodent SXRs share ~95% amino acid sequence identity in the DNA-binding domain (DBD) but only about 77% identity in the LBD. Tirona *et al.* (2004) analyzed the ligand selectivity of a human-rat chimeric protein and showed that the species differences are primarily defined by sequence differences in the LBD. Watkins and colleagues showed that the key residues responsible for the majority of the ligand selectivity were Leu 308 (human) and Phe305 (rat and mouse). Crystallographic analysis located these amino acids within or neighboring the flexible loop that forms a part of the pore to the ligand-binding cavity. Swapping the rodent and human-specific residues was shown to modulate the activation by the human-selective activator RIF *in vitro* (Watkins *et al.*, 2001). According to those findings, a simple replacement of the mouse LBD with the human sequence should be sufficient to "humanize" the ligand binding properties as well as activation of the downstream target genes.

Three kinds of humanized mice have already been generated. One is the SXR-null/Alb-SXR mouse (Alb-SXR mouse) made by crossing the SXR knockout mice with a transgenic mouse line that expresses human SXR in liver under the control of the albumin promoter (Xie *et al.*, 2000). Gonzalez and colleagues generated a transgenic mouse expressing a human BAC containing the entire hSXR gene in a SXR null background, thus controlled under human SXR promoter (SXR BAC mouse) (Ma *et al.*, 2007). Another mouse is the human SXR genome knock-in mice (hSXR genome mouse) (Scheer *et al.*, 2008). The human SXR genomic region from exon 2 to exon 9 was knocked-in to mouse SXR exon 2. This mouse expresses the human full length SXR mRNA under the control of mouse SXR promoter regulation. Although useful for toxicology studies, these mice have disadvantages in that the human SXR is expressed only in the liver (Alb-SXR mouse), hSXR mRNA is not expressed in all of the tissues where SXR is known to be expressed (SXR BAC mouse), and there might be potential differences in the binding affinities of hSXR DNA-binding domain (DBD) to *cis*-acting elements in mouse SXR target genes (hSXR genome mouse).

As noted above, it is known that the critical differences between human and rodent ligand-selectivity reside in the LBD. Therefore, when our project to generate a humanized SXR mouse was initiated, we reasoned that altering the LBD would be sufficient to generate a humanized ligand selectivity. We decided to retain the mouse DBD to avoid any potential differences between the binding affinities of the chimeric receptor for cis-acting elements in the mouse genome. To maintain the tissue-specific expression pattern of the endogenous gene, we inserted the human cDNA encoding the region carboxyl-terminal to the DBD into the mouse gene. This retains all of the 5' and 3' regulatory elements in the mouse gene, as well as introns 1 and 2, which contain important elements for regulating SXR expression (Jung *et al.*, 2006).

Here we report a new line of mouse (hSXRki mouse) in which a cDNA encoding the human LBD is homologously recombined into the mouse gene after exon 3. The tissue distribution of the resulting chimeric mouse DBD-human LBD mRNA is comparable to that of the WT mouse. The hSXRki mouse showed a fully humanized response to the human-selective activator RIF in that the Cyp3a11 mRNA was induced in liver and mucosa of small intestine in response to RIF, but not the rodent-selective compound PCN. This new mouse line should provide a useful tool for assessing the whole body toxicity induced by a human selective SXR ligand itself and its subsequently generated metabolite(s) that can trigger further toxic responses through other pathways body-wide.

MATERIALS AND METHODS

Generation of hSXRki knock-in mice

A DNA fragment of mouse SXR intron 2 to exon 3 was PCR amplified using mouse BAC DNA (BAC clone No. RP23-351P21) as a template. Primers used were BAC39486FW and mSXR462RV (for sequences of the primers see Table1). This fragment was connected to the LBD of human SXR cDNA from amino acid 105 through the carboxyl terminus amplified by the PCR primers: hSXR904FW and hSXR1887RVEcoR1 (template; human SXR cDNA). The 3'UTR of bovine growth hormone (BGH) was added to 3' to the terminal codon. This concatenated fragment was introduced to a vector, which

Table 1. List of primer pairs

Purpose	Primer name	Sequence (5' to 3')
Targeting vector construction	BAC39486FW	CCATGGGTACCACGAATAACAA
	mSXR462RV	CATGCCACTCTCCAGGCA
	hSXR904FW	AAGAAGGAGATGATCATGTCCG
	hSXR1887RVEcoRI	CCGAATTCTCATCATCAGCTACCTGTGATACCGAACA
Genotyping	NeoAL2	GGGGATGCGGTGGGCTCTATGGCTT
	SXR RC RV5	TGAGAGTGCACAAGTTCAAGCT
	WTInt5	AGTGATGGGAACCACTCCTG
	WTEx6RV	TGGTCCTCAATAGGCAGGTC
	mhSXRE4	GTGAACGGACAGGGACTCAG
	mhSXRSARV	CTCTCCTGGCTCATCCTCAC
Percellome quantitative RT-PCR	Cyp3a11 FW	CAGCTTGGTGCTCCTCTACC
	Cyp3a11 RV	TCAAACAACCCCCATGTTTT
	Ces6 FW	GGAGCCTGAGTTCAGGACAGAC
	Ces6 RV	ACCCTCACTGTTGGGGTTC
	mouse SXR FW	AATCATGAAAGACAGGGTTC
	mouse SXR RV	AAGAGCACAGATCTTTCCG
	human SXR FW	ATCACCCGGAAGACACGAC
	human SXR RV	AAGAGCACAGATCTTTCCG
	mouse-human SXR FW	CCCATCAACGTAGAGGAGGA

has the neomycin resistance gene with loxP sequence at both ends, removable with Cre recombinase (Saga *et al.*, 1999). A 7kb KpnI fragment containing intron 2 was used as a long arm and 1.3kb PstI-EcoRI fragment containing from exon 8 to intron 8 was used as a short arm for homologous recombination (Fig. 1). The resulting targeting vector was linearized with SacII and introduced by electroporation to TT2 ES cell line (Yagi *et al.*, 1993) and neomycin resistant clones were selected, PCR genotyped, and confirmed by the Southern blotting. For generation of chimeric mice, these ES clones were aggregated with ICR 8-cell embryos and transferred to pseudopregnant female recipients. The chimeric mice born were bred with ICR females. Germ line transmission of the targeted allele was confirmed by PCR. A mouse was crossed with a CAG-Cre transgenic mouse (Sakai and Miyazaki, 1997) to evict the neomycin resistance gene, and back crossed to C57BL/6 CrSlc (SLC, Inc., Shizuoka, Japan) at least 6 generations and used for the analysis.

PCR Genotyping
(See Table 1 for primer sequences)

Primers for identification of homologously recombined ES clones were NeoAL2 and SXR RC RV5. DNA purified from the tail of each mouse was used for PCR genotying. Primers for WT detection were WTInt5 and WTEx6RV amplifying a product of 755 bp. Primers for confirmation of removal of the neomycin resistance gene were mhSXRE4 and mhSXRSARV amplifying a product of 1,223 bp.

Southern blot analysis

To confirm homologous recombination, DNA from ES cell cultures was purified and digested with BamHI and XhoI, then electrophoresed and analyzed by Southern hybridization (Saga *et al.*, 1997). Mouse SXR exon 9 region which remains after homologous recombination was used for the probe. The restriction fragments from the WT allele and targeted allele are 2,305 bp and 1,925 bp, respectively.

Chemicals

RIF (molecular weight 822.95) and PCN (molecular weight 341.49) were purchased from Sigma-Aldrich (St. Louis, MO, USA). Corn oil was purchased from Wako Pure Chemical Industries (Osaka, Japan).

Quantitative RT-PCR (Percellome PCR)
(See Table 1 for primer sequences)

The method for Percellome quantitative RT-PCR was described previously (Kanno *et al.*, 2006). Briefly, tissue pieces stored in RNAlater (Ambion, Austin, TX, USA) were homogenized and lysed in RLT buffer (Qiagen GmbH., Germany) and 10 µl aliquots were used

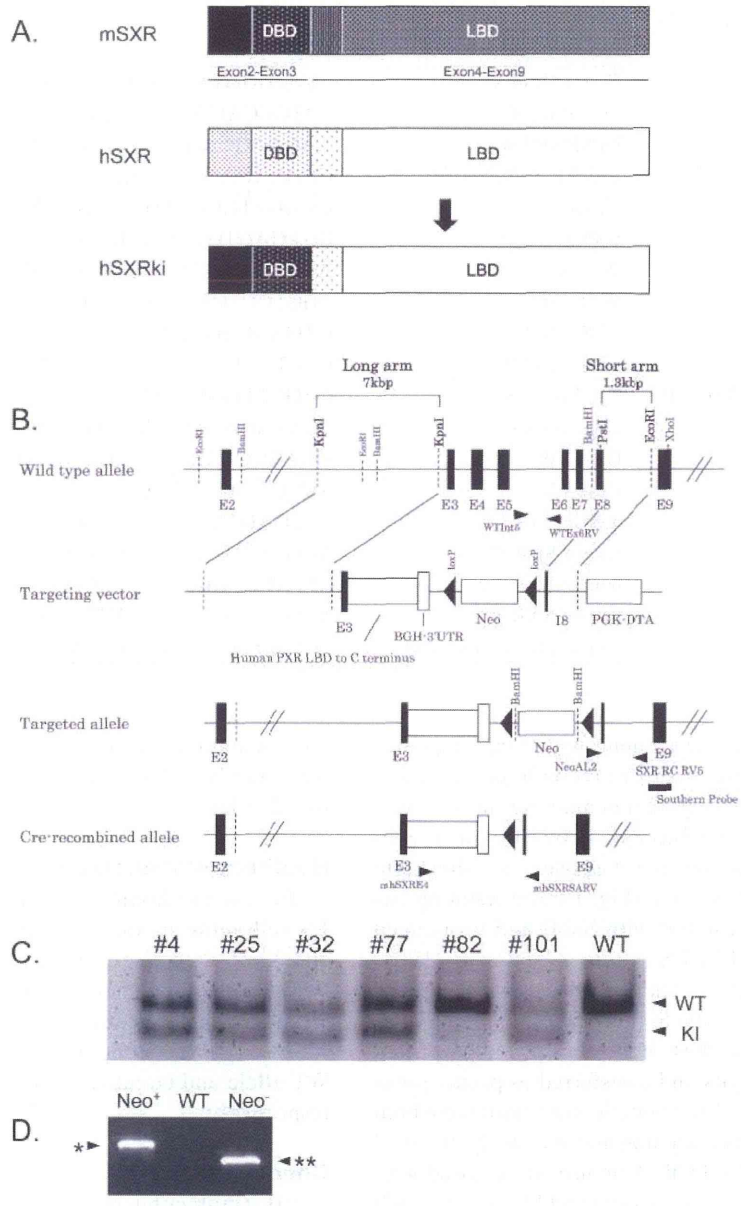

Fig. 1. Targeting strategy used to generate the hSXRki mouse. A) Diagram of hSXRki chimeric protein. Hinge region and ligand binding domain (LBD) of human SXR are knocked-in to mouse SXR, resulting in chimeric protein having murine N-ternial domain and DNA binding domain (DBD). B) Targeting strategy used to generate the hSXRki mouse. The chimeric mouse DBD and human LBD fragment, followed by the BGH 3' UTR were knocked-in to the mouse SXR gene. The genomic region spanning from exon 3 to exon 8 was substituted by the inserted fragment with the remainder of the gene remaining intact. C) Confirmation of homologous recombination by southern blot analysis. Six ES clones positive for recombination by PCR genotyping were further analyzed by southern blot (clones #4 ~ #101). Lower bands (1925 bp) indicate successful homologous recombination; upper bands (2305 bp) correspond to WT allele. Clones #4, #25, #32, #77 and #101 were confirmed as homologous recombinants; clones #4 and #25 were used for the generation of chimeric mice. D) Confirmation of Cre-mediated removal of the neomycin resistance gene. Mouse tail genome DNA was PCR amplified with the primer set, mhSXRE4 and mhSXRSARV. *: 2,858 bp (for the mice having the neomycin resistance gene), **: 1,223 bp (for the mice without the neomycin resistance gene).

for genomic DNA quantification with PicoGreen fluorescent dye (Invitrogen, Carlsbad, CA, USA). A prepared spike mRNA cocktail solution containing known quantity of five mRNAs of bacillus subtilis was added to the tissue lysate in proportion to the DNA quantity. Total RNA was purified from the lysate using the RNeasy kit (Qiagen). One microgram of total RNA was reverse-transcribed with SuperScript II (Invitrogen). Quantitative real time PCR was performed with an ABI PRISM 7900 HT sequence detection system (Applied Biosystems) using SYBR Green PCR Master Mix (Applied Biosystems), with initial denaturation at 95°C for 10 min followed by 40 cycles of 30 sec at 95°C and 30 sec at 60°C and 30 sec at 72°C, and Ct values were obtained. Primers for Cyp3a11 were Cyp3a11 FW and Cyp3a11 RV. Primers for Ces6 were Ces6 FW and Ces6 RV. Primers for mouse SXR selective quantification were mouse SXR FW and mouse SXR RV. Primers for hSXRki selective quantification were human SXR FW and human SXR RV. Primers for both mouse SXR and hSXRki quantification were mouse-human SXR FW and mouse-human SXR RV that amplify the DBD region of the chimera.

In Situ Hybridization analysis

Digoxigein-labeled cRNA probe for Cyp3a11 was synthesized according to Suzuki *et al.* (2005) by RT-PCR using mouse liver cDNA as a template. The primers used were as follows: forward 5'-GATTGGTTTTGATGCCTGGT-3' and reverse 5'-CAAGAGCTCACATTTTTCATCA-3'. The amplified product was sequence confirmed and ligated with Block-iT T7-TOPO (Invitrogen) Linker, which contains the T7 promoter site. A secondary PCR was performed to generate the sense and antisense DNA templates. For antisense template, Block-iT T7 Primer and Cyp3a11 forward primer (or reverse primer for generation of sense DNA template), the same primer as for the first PCR amplification, were used. With these DNA templates, both sense and antisense digoxigenin-labeled riboprobes were synthesized using a DIG RNA labeling kit (Roche Diagnostics, Germany) according to the manufacturer's protocol.

ISH on paraffin sections was carried out according to Suzuki *et al.* with a modification; permeabilization condition 98°C for 15 min in HistoVT One (Nacalai tesque, Japan).

Animals experiments

Male hSXRki and WT mice were maintained under a 12 hr light/12 hr dark cycle with water and chow (CRF-1, Oriental Yeast Co. Ltd., Tokyo, Japan) provided *ad libitum*. The animal studies were conducted in accordance with the Guidance for Animal Studies of the National Institute of Health Sciences under Institutional approval. The expression level of the hSXRki and WT SXR mRNA of ten organs (brain, thymus, heart, lung, liver, stomach, spleen, kidney, small intestine and testis) were analyzed on 15 weeks old male mice (n = 2) by the Percellome quantitative RT-PCR.

For the demonstration of selective gene induction by RIF and PCN in hSXRki and WT male mice on 13 weeks

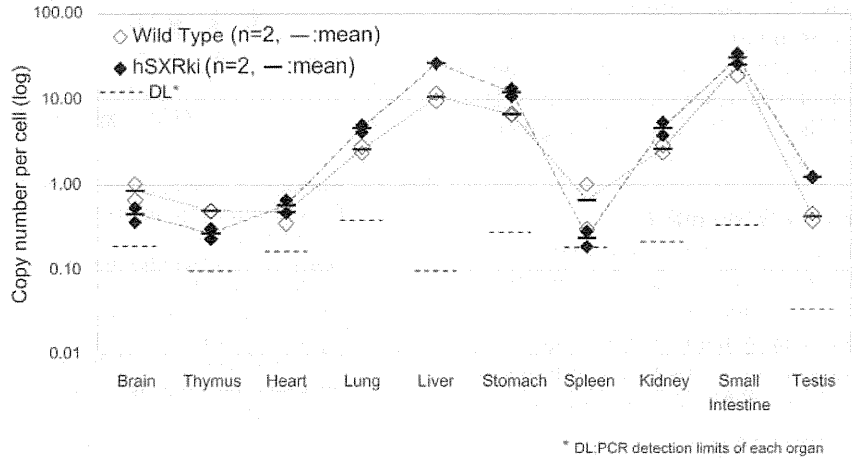

Fig. 2. Conservation of tissue expression patterns of hSXRki mRNA in the knock-in mouse. Percellome quantitative RT-PCR analysis was performed to measure the absolute expression levels of WT SXR mRNA and hSXRki mRNA in ten organs of WT and hSXRki mice. The expression levels of hSXRki mRNA among organs were comparable to WT.

old, three mice per group were singly dosed orally with vehicle (corn oil+0.1% DMSO), 10, 30, or 100 mg/kg of RIF, or 20, 70, or 200 mg/kg PCN (approximately equivalent in molar dose). Eight hours later, mice were sacrificed by exsanguination under ether anesthesia and the liver and the small intestine mucosa were sampled. Liver samples in small pieces were stored in RNA later (Applied Biosystems, Foster City, CA, USA) for further analysis. The small intestine under ice-cooled condition was longitudinally opened, gently rinsed with RNase-free saline and the epithelium was scraped with a glass slide and immersed in RNAlater. For *in situ* hybridization (ISH) of Cyp3a11 in the liver, 15 weeks old male hSXRki and WT mice were dosed orally with vehicle (corn oil), RIF (10 mg/kg), or PCN (40 mg/kg) daily for 3 days and liver sampled 24 hr later. All mice were sacrificed by exsanguination under ether anesthesia.

Statistical analysis

All values are expressed as the means ± S.D. and group differences analyzed by unpaired Student's *t* test or one-way ANOVA followed by Dunnett's post hoc comparison. Level of significance was set at $p < 0.05$.

RESULTS

Generation of hSXRki knock-In mice

Among 144 neomycin resistant TT2 ES clones, six PCR positive clones were further submitted to Southern blotting for the confirmation of homologous recombination. As shown in Fig. 1C, five clones were confirmed, and two (#4 and #25) were used to generate chimeric mice. The resulting mice were backcrossed to ICR strain to confirm germline transmission. One clone (#4) was crossed to a mouse constitutively expressing Cre recombinase to remove the neomycin resistance gene (Fig. 1D) and backcrossed to C57BL/6 CrSlc for at least 6 generations before further analysis.

Tissue distribution of hSXRki mRNA

Ten tissues, i.e., brain, thymus, heart, lung, liver, stomach, spleen, kidney, small intestine and testis from both hSXRki and WT mice were measured for hSXRki or WT SXR mRNA expression by the Percellome quantitative RT-PCR. As shown in Fig. 2, the levels of hSXRki mRNA are comparable to that of SXR in WT mouse and expressed in all tissues analyzed.

Humanized responses in hSXRki mouse

Humanized response of hSXRki was demonstrated by administration of the mouse-specific ligand PCN and the

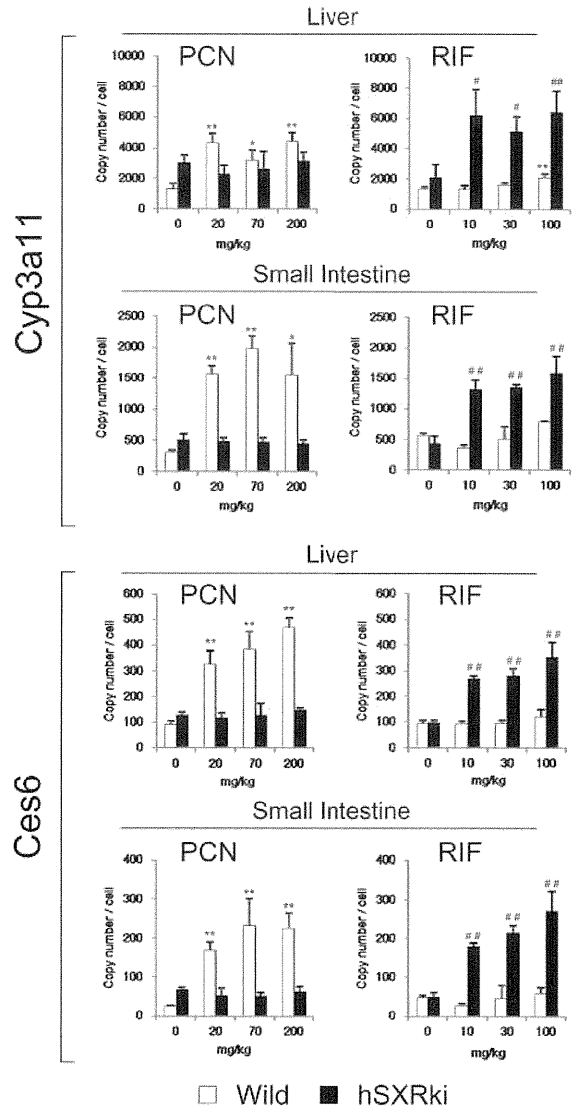

Fig. 3. Humanized response of hSXRki mice to RIF and PCN; Percellome quantitative RT-PCR. WT mice and hSXRki mice (n = 3 each) were singly dosed orally with vehicle (corn oil+0.1% DMSO), 20, 70, or 200 mg/kg PCN, or 10, 30, or 100 mg/kg of RIF (approximately equivalent in molar dose each other). Percellome quantitative RT-PCR data of Cyp3a11 and Ces6, both known as SXR target genes, in liver and small intestinal mucosa showed humanized responses in hSXRki. Bars = S.D., *; $p < 0.05$, **; $p < 0.01$ compared with vehicle group of WT, #; $p < 0.05$, ##; $p < 0.01$ compared with vehicle group of hSXRki. Analyzed by one-way ANOVA followed by Dunnett's post hoc comparison. Level of significance was set at $p < 0.05$.

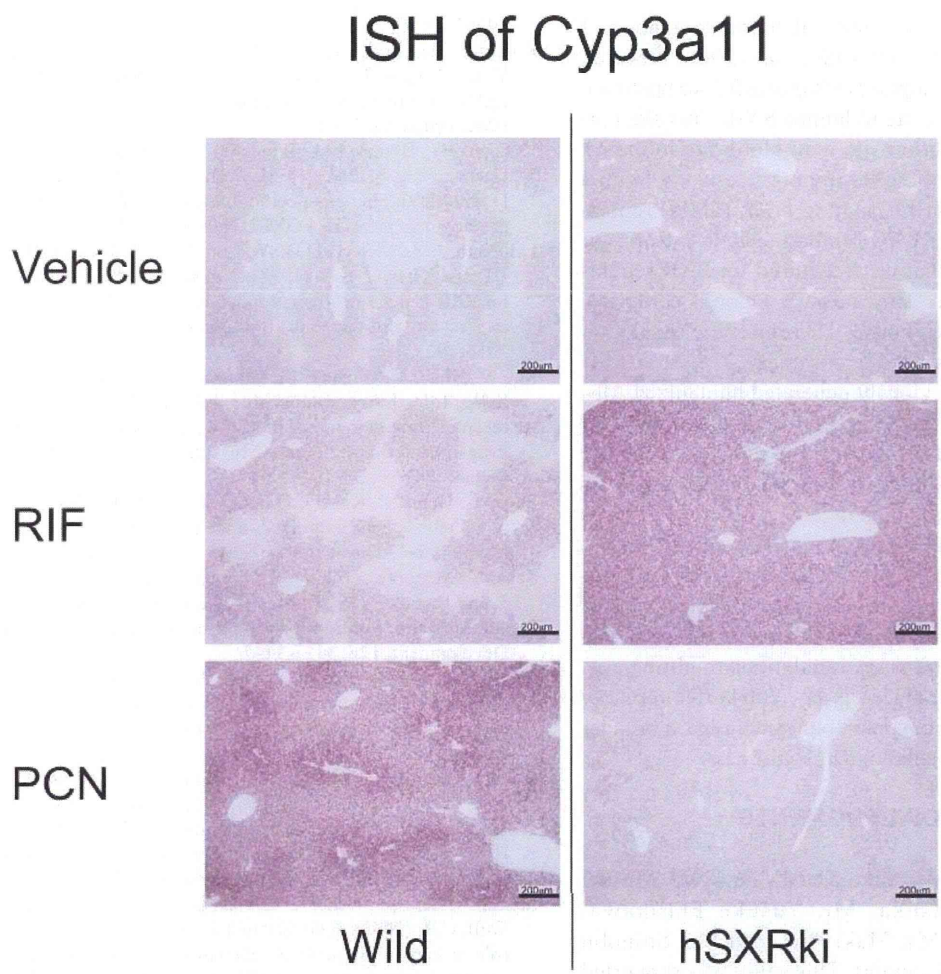

Fig. 4. Humanized response of hSXRki mice to RIF and PCN: *In situ* hybridization for Cyp3a11 mRNA in liver. A DIG-labeled cRNA probe for Cyp3a11 was hybridized and developed for purplish blue chromogenic reaction. Histologically, Cyp3a11 induction was localized around the central veins in both mice with species-specific ligands, respectively.

human-specific ligand RIF to the mice. Induction of the well-known SXR-regulated genes, Cyp3a11 and Ces6 was monitored by Percellome quantitative RT-PCR. As shown in Fig. 3, in the liver and small intestinal mucosa, RIF, but not PCN, induced Cyp3a11 and Ces6 in hSXRki mice (closed column), whereas PCN exclusively induced these genes in WT mice (open column). ISH of Cyp3a11 of the liver also showed humanized responses in hSXRki mice (Fig. 4).

DISCUSSION

We generated a new humanized mouse model in which the ligand binding domain (LBD) of human SXR was homologously knocked-into the murine SXR gene so that systemic response induced by human-selective SXR ligands can be monitored in mice. Firstly, we showed that mRNA from this chimeric gene was expressed at appropriate levels in the same tissues as the endogenous mouse SXR gene in WT mice. Then the humanized response of the mouse was confirmed by monitoring its response to the human-selective activator RIF, and the lack of response to the rodent-selective activator PCN.

There are relatively few reports about the regulation of SXR expression to date. Aouabdi *et al.* (2006) reported the presence of a PPAR alpha binding site 2.2 kb upstream of the transcription start site in human SXR. This site corresponded to the induction site with clofibrate in the rat and they further confirmed its importance using human liver cancer cell line (Huh7). Jung *et al.* (2006) reported the presence of four FXR binding sites in intron 2 of the mouse SXR gene that were required for FXR regulation of SXR expression. This intron 2 region is completely intact in our hSXRki mouse. Therefore, the regulation by FXR should be preserved in our mice.

Compared to the previously generated humanized Alb-SXR, SXR BAC, and hSXR genome mice, we contend that our hSXRki mouse has an advantage because the human-mouse chimeric gene is expressed in the same tissues and at similar levels to endogenous SXR in WT mice under control of the mouse promoter. This feature would make this model suitable not only for systemic toxicity but also toxicity at various stages of development of the embryo and fetus, maturation of infant, and of senescence, where the *cis* and *trans* regulations might be critical in its regulation (Sarsero *et al.*, 2004) (Konopka *et al.*, 2009). Thus, we believe that our system has a broader application range for toxicological studies.

ACKNOWLEDGMENTS

The authors thank Ms. Yuko Matsushima, Mr. Masaki Tsuji, Ms. Maki Otsuka, Mr. Yusuke Furukawa, Mr. Kouichi Morita, Ms. Maki Abe, and Ms. Shinobu Watanabe for technical support. This study was supported in part by the Health Sciences Research Grants H19-Tox-ico-Shitei-001 from the Ministry of Health, Labour and Welfare, Japan.

REFERENCES

Aouabdi, S., Gibson, G. and Plant, N. (2006): Transcriptional regulation of the PXR gene: identification and characterization of a functional peroxisome proliferator-activated receptor alpha binding site within the proximal promoter of PXR. Drug Metab. Dispos., **34**, 138-144.

Bertilsson, G., Heidrich, J., Svensson, K., Asman, M., Jendeberg, L., Sydow-Bäckman, M., Ohlsson, R., Postlind, H., Blomquist, P. and Berkenstam, A. (1998): Identification of a human nuclear receptor defines a new signaling pathway for CYP3A induction. Proc. Natl. Acad. Sci., USA, **95**, 12208-12213.

Blumberg, B., Sabbagh, W.Jr., Juguilon, H., Bolado, J.Jr., van Meter, C.M., Ong, E.S. and Evans, R.M. (1998): SXR, a novel steroid and xenobiotic-sensing nuclear receptor. Genes. Dev., **12**, 3195-3205.

Jung, D., Mangelsdorf, D.J. and Meyer, U.A. (2006): Pregnane X receptor is a target of farnesoid X receptor. J. Biol. Chem., **281**, 19081-19091.

Kanno, J., Aisaki, K., Igarashi, K., Nakatsu, N., Ono, A., Kodama, Y. and Nagao, T. (2006): "Per cell" normalization method for mRNA measurement by quantitative PCR and microarrays. BMC genomics, **7**, 64.

Konopka, G., Bomar, J.M., Winden, K., Coppola, G., Jonsson, Z.O., Gao, F., Peng, S., Preuss, T.M., Wohlschlegel, J.A. and Geschwind, D.H. (2009): Human-specific transcriptional regulation of CNS development genes by FOXP2. Nature, **462**, 213-217.

Lehmann, J.M., McKee, D.D., Watson, M.A., Willson, T.M., Moore, J.T. and Kliewer, S.A. (1998): The human orphan nuclear receptor PXR is activated by compounds that regulate CYP3A4 gene expression and cause drug interactions. J. Clin. Invest., **102**, 1016-1023.

Ma, X., Shah, Y., Cheung, C., Guo, G.L., Feigenbaum, L., Krausz, K.W., Idle, J.R. and Gonzalez, F.J. (2007): The PREgnane X receptor gene-humanized mouse: a model for investigating drug-drug interactions mediated by cytochromes P450 3A. Drug Metab. Dispos., **35**, 194-200.

Saga, Y., Hata, N., Koseki, H. and Taketo, M.M. (1997): Mesp2: a novel mouse gene expressed in the presegmented mesoderm and essential for segmentation initiation. Genes. Dev., **11**, 1827-1839.

Saga, Y., Miyagawa-Tomita, S., Takagi, A., Kitajima, S., Miyazaki, J. and Inoue, T. (1999): MesP1 is expressed in the heart precursor cells and required for the formation of a single heart tube. Development, **126**, 3437-3447.

Sakai, K. and Miyazaki, J. (1997): A transgenic mouse line that retains Cre recombinase activity in mature oocytes irrespective of the cre transgene transmission. Biochem. Biophys. Res. Commun., **237**, 318-324.

Sarsero, J.P., Li, L., Holloway, T.P., Voullaire, L., Gazeas, S., Fowler, K.J., Kirby, D.M., Thorburn, D.R., Galle, A., Cheema, S., Koenig, M., Williamson, R. and Ioannou, P.A. (2004): Human BAC-mediated rescue of the Friedreich ataxia knockout mutation in transgenic mice. Mamm. Genome., **15**, 370-382.

Scheer, N., Ross, J., Rode, A., Zevnik, B., Niehaves, S., Faust, N. and Wolf, C.R. (2008): A novel panel of mouse models to evaluate the role of human pregnane X receptor and constitutive androstane receptor in drug response. J. Clin. Invest., **118**, 3228-3239.

Suzuki, T., Akimoto, M., Mandai, M., Takahashi, M. and Yoshimura, N. (2005): A new PCR-based approach for the preparation of RNA probe. J. Biochem. Biophys. Methods., **62**, 251-258.

Tirona, R.G., Leake, B.F., Podust, L.M. and Kim, R.B. (2004): Identification of amino acids in rat pregnane X receptor that determine species-specific activation. Mol. Pharmacol., **65**, 36-44.

Watkins, R.E., Wisely, G.B., Moore, L.B., Collins, J.L., Lambert, M.H., Williams, S.P., Willson, T.M., Kliewer, S.A. and Redinbo, M.R. (2001): The human nuclear xenobiotic receptor PXR: structural determinants of directed promiscuity. Science, **292**, 2329-2333.

Xie, W., Barwick, J.L., Downes, M., Blumberg, B., Simon, C.M., Nelson, M.C., Neuschwander-Tetri, B.A., Brunt, E.M., Guzelian, P.S. and Evans, R.M. (2000): Humanized xenobiotic response in mice expressing nuclear receptor SXR. Nature, **406**, 435-439.

Yagi, T., Tokunaga, T., Furuta, Y., Nada, S., Yoshida, M., Tsukada, T., Saga, Y., Takeda, N., Ikawa, Y. and Aizawa, S. (1993): A novel ES cell line, TT2, with high germline-differentiating potency. Anal. Biochem., **214**, 70-76.

Zhou, C., Tabb, M.M., Sadatrafiei, A., Grün, F. and Blumberg, B. (2004) Tocotrienols activate the steroid and xenobiotic receptor, SXR, and selectively regulate expression of its target genes. Drug Metab. Dispos., **32**, 1075-1082.

OPEN ACCESS Freely available online

PLoS one

Analysis of Factors Lowering Sensitivity of Interferon-γ Release Assay for Tuberculosis

Nguyen Thi Le Hang[1], Luu Thi Lien[2], Nobuyuki Kobayashi[3], Takuro Shimbo[4], Shinsaku Sakurada[5], Pham Huu Thuong[2], Le Thi Hong[6], Do Bang Tam[6], Minako Hijikata[5], Ikumi Matsushita[5], Nguyen Van Hung[7], Kazue Higuchi[8], Nobuyuki Harada[8], Naoto Keicho[5]*

1 NCGM-BMH Medical Collaboration Center, Hanoi, Viet Nam, **2** Hanoi Lung Hospital, Hanoi, Viet Nam, **3** Department of Respiratory Medicine, National Center for Global Health and Medicine, Tokyo, Japan, **4** Department of Clinical Research and Informatics, International Clinical Research Center, National Center for Global Health and Medicine, Tokyo, Japan, **5** Department of Respiratory Diseases, Research Institute, National Center for Global Health and Medicine, Tokyo, Japan, **6** Department of Biochemistry, Hematology and Blood Transfusion, Hanoi Lung Hospital, Hanoi, Viet Nam, **7** Department of Bacteriology, National Lung Hospital, Hanoi, Viet Nam, **8** Department of Mycobacterium Reference and Research, Research Institute of Tuberculosis, Tokyo, Japan

Abstract

Background: Imperfect sensitivity of interferon-γ release assay (IGRA) is a potential problem to detect tuberculosis. We made a thorough investigation of the factors that can lead to false negativity of IGRA.

Methods: We recruited 543 patients with new smear-positive pulmonary tuberculosis in Hanoi, Viet Nam. At diagnosis, peripheral blood was collected and IGRA (QuantiFERON-TB Gold In-Tube) was performed. Clinical and epidemiological information of the host and pathogen was collected. The test sensitivity was calculated and factors negatively influencing IGRA results were evaluated using a logistic regression model in 504 patients with culture-confirmed pulmonary tuberculosis.

Results: The overall sensitivity of IGRA was 92.3% (95% CI, 89.6%–94.4%). The proportions of IGRA-negative and -indeterminate results were 4.8% (95% CI, 3.1%–7.0%) and 3.0% (95% CI, 1.7%–4.9%). Age increased by year, body mass index <16.0, HIV co-infection and the increased number of HLA-DRB1*0701 allele that patients bear showed significant associations with IGRA negativity (OR = 1.04 [95% CI, 1.01–1.07], 5.42 [1.48–19.79], 6.38 [1.78–22.92] and 5.09 [2.31–11.22], respectively). HIV co-infection and the same HLA allele were also associated with indeterminate results (OR = 99.59 [95% CI, 15.58–625.61] and 4.25 [1.27–14.16]).

Conclusions: Aging, emaciation, HIV co-infection and HLA genotype affected IGRA results. Assessment of these factors might contribute to a better understanding of the assay.

Citation: Hang NTL, Lien LT, Kobayashi N, Shimbo T, Sakurada S, et al. (2011) Analysis of Factors Lowering Sensitivity of Interferon-γ Release Assay for Tuberculosis. PLoS ONE 6(8): e23806. doi:10.1371/journal.pone.0023806

Editor: Pere-Joan Cardona, Fundació Institut Germans Trias i Pujol; Universitat Autònoma de Barcelona CibeRES, Spain

Received May 6, 2011; **Accepted** July 25, 2011; **Published** August 19, 2011

Copyright: © 2011 Hang et al. This is an open-access article distributed under the terms of the Creative Commons Attribution License, which permits unrestricted use, distribution, and reproduction in any medium, provided the original author and source are credited.

Funding: This work was supported by a grant from the program of the Japan Initiative for Global Research Network on Infectious Diseases (J-GRID), MEXT, Japan. The funder had no role in study design, data collection and analysis, decision to publish, or preparation of the manuscript.

Competing Interests: The authors have declared that no competing interests exist.

* E-mail: nkeicho-tky@umin.ac.jp

Introduction

Tuberculosis (TB) remains a disease of serious concern: one third of the global population is infected with *Mycobacterium tuberculosis* (MTB) and eight to ten million people develop the disease every year [1]. The primary step to control TB is detecting infection by a sensitive test.

Recently, an immunoassay that measures interferon (IFN)-γ response to MTB-specific antigens (interferon-γ release assay; IGRA) has been developed. Studies on the use of IGRA in patients with active TB have had two purposes: (1) to evaluate performance of IGRA in latent TB infection (LTBI) using active TB as a surrogate, and (2) to determine whether IGRA plays a supplementary role in the exclusion of active TB disease in optimal setting [2–4].

IGRA use in diagnosis of LTBI has been established and supported by European and American guidelines [5,6], whereas its use has not been recommended to rule out active disease particularly in high-burden countries, because of low sensitivity and low negative predictive values [7,8]. Consequently, so far the sensitivity of IGRA varies from 64% to 92% [3], but the number of reports from high-burden countries is limited.

Imperfect sensitivity is a potential problem when using this assay to exclude LTBI as well as active TB. Due to the lack of a gold standard for LTBI identification, mechanisms by which IGRA gives false-negative results in LTBI are largely unknown [2,3]. Identification and characterization of factors that lower the test sensitivity, by using active TB patients as a surrogate for LTBI suspects, would delineate active TB-disease specific and non-specific mechanisms that underlie false negative results of IGRA.

At present, however, there is no comprehensive report on relevant factors including extent of TB lesions, malnutrition, aging, HIV co-infection, and MTB strains. Inherent genetic variations are also candidate factors affecting IGRA results. Among these, polymorphism of human leukocyte antigen (HLA) is classically known to influence T-cell immune response and determines IFN-γ concentrations after stimulation with MTB antigens [9]. In this study, we thus attempted to investigate host- and pathogen-related factors that may influence IGRA results obtained from more than 500 patients with active TB in Viet Nam.

Methods

Ethics statement

A written informed consent was obtained from each participant. The study was approved by ethical committees of the Ministry of Health, Viet Nam and National Center for Global Health and Medicine, Japan respectively.

Study population

This study is a part of our prospective study on active TB in Hanoi. After signing informed consents, 543 unrelated patients with smear-positive pulmonary TB, equal to or more than 16 years of age, and without history of TB treatment, entered this study from July 2007 to March 2009. Information of no previous TB treatment was based on self-declaration of patients and documents in district TB centers.

All had sputum smear-positive TB. Solid MTB culture on Löwenstein-Jensen media was available in 98.2% and confirmed the diagnosis in 504 patients (92.8%). The sensitivity and risk-factor analysis was made in these culture-confirmed pulmonary TB cases, although clinicians diagnosed all 543 patients as active pulmonary TB and treated them with anti-TB drugs based on the guidelines of the national TB program. Spoligotyping was used to distinguish MTB genotypes including Beijing strains [10]. At diagnosis before anti-TB treatment, the peripheral blood was drawn for testing complete blood count, HIV, IGRA and HLA genotyping. After 2 months of treatment, IGRA was tested again. Chest X-ray films were interpreted by two readers independently of IGRA results.

IGRA

In this study, ELISA-based IGRA, QuantiFERON-TB Gold In-Tube™ (QFT-IT) (Cellestis, Victoria, Australia), was used [11]. The algorithm and software (QuantiFERON-TB Gold Analysis Software, version 2.50, Cellestis) provided by the manufacturer were strictly followed for interpretation of the results [11]. The testing procedure was carefully monitored [12] and quality control of the test was done in each run, following the manufacturer's instructions. For analysis of IFN-γ values higher than 10.00 IU/ml, the truncated value (10.00 IU/ml) was used as indicated in the current software.

HLA typing

Genomic DNA was extracted from the whole blood by using the QIAamp™ DNA Blood Midi Kit (QIAGEN Sciences, Germantown, MD, USA). DNA-based HLA typing was performed by Luminex Multi-Analyte Profiling system (xMAP) with WAKFlow HLA typing kit (Wakunaga, Hiroshima, Japan) as described [13]. Briefly, highly polymorphic exon 2 of HLA-DRB1 and -DQB1 genes were amplified. Each PCR product was hybridized with sequence-specific oligonucleotide probes, complementary to the allele-specific sequences.

Linkage disequilibrium analysis and binding peptide prediction for HLA alleles

Haploview version 4.2 (Broad Institute, Cambridge, MA) was used to calculate indicators of linkage disequilibrium, D' and r^2, between HLA-DRB1 and -DQB1 alleles [14,15].

To predict peptides in the protein sequence of ESAT-6, CFP10 and TB7.7 capable of binding to a given HLA-DRB1 allele *in silico*, we used the ProPred database [16,17] with a threshold of 3%, a recommended setting.

Statistical analysis

Factors negatively influencing IGRA results were initially screened by univariate analysis and then further investigated by multivariate analysis using a polytomous logistic regression model, with IGRA-negative and -indeterminate results as outcome variables and factors that may be involved in host immunity and disease as independent variables. Another logistic regression model using a dichotomous outcome variable, non-positive (negative and indeterminate) versus positive results, was also tested. Odd ratio (OR) and 95% confidential interval (CI) were thus calculated. HLA candidate alleles were initially screened by comparison of allele frequencies between IGRA-negative and -positive groups, and then further investigated by the logistic regression model mentioned above.

Fisher's exact test was used to detect associations. Bonferroni's correction was applied to correct multiple comparisons of association with HLA alleles. Distribution of IFN-γ values was represented by using median with interquartile range (IQR). When a value was higher than 10.00 IU/ml, truncated values (10.00 IU/ml) were presented and a quantile value based on extrapolation was supplied only as parenthetical. Wilcoxon rank-sum test and Kruskal-Wallis test were used to compare non-parametric distribution of two groups and more than two groups, respectively. P value <0.05 was considered to be statistically significant, unless otherwise specified. Statistical analysis was performed using Stata version 10 (StataCorp, College Station, TX).

Results

Characteristic of the study population

Data including QFT-IT results were analyzed in 504 new patients with culture-confirmed pulmonary TB. The median age was 38.8, the proportion of male patients was 79.2%, and HIV was positive in 8.7% of the cases. Body mass index (BMI) showed that more than 50% of the patients were underweight, following the categorization on the basis of international guidelines [18] (table 1).

QFT-IT results

In 504 patients tested, the overall sensitivity of QFT-IT was 92.3% (95% CI, 89.6%–94.4%), but decreased to 61.4% (95% CI, 45.5%–75.6%) in HIV-infected patients (table 2). The proportions of QFT-IT-negative and -indeterminate results were 4.8% (95% CI, 3.1%–7.0%) and 3.0% (95% CI, 1.7%–4.9%) respectively. All of the 15 indeterminate cases had low response to phytohaemagglutinin (PHA, or mitogen) and TB-Ag after subtracting Nil value (TBAg-Nil) (0.20 [IQR, 0.04–0.34] IU/ml and 0.03 [IQR, 0.01–0.06] IU/ml, respectively). Compared with the patients who had test-positive results, those with negative results were significantly older (median age: 48.9 [IQR, 33.2–62.6] vs 39.0 [IQR, 29.1–50.6], $P=0.036$), and had significantly lower BMI (median BMI: 16.6 [IQR, 13.9–17.9] vs 18.3 [16.9–19.7] kg/m^2, $P=0.0001$) (table not shown).

Table 1. Characteristics of patients with smear-positive/culture-positive pulmonary tuberculosis (n = 504).

		Number	%
Age (years old) (median, IQR)		(38.8,	29.2–50.8)
Sex	Male	399	79.2
	Female	105	20.8
Body mass index	<16.0	77	15.3
	16.0–18.4	206	40.9
	18.5–24.9	218	43.2
	≥25.0	3	0.6
Smoking habit	Smoker	199	39.5
	Ex-smoker	136	27.0
	Non-smoker	168	33.3
	No answer	1	0.2
Underlying disease other than HIV*	None	435	86.3
	One	61	12.1
	More than one	8	1.6
HIV status	Positive	44	8.7
	Negative	459	91.1
	Not available	1	0.2
Lymphocyte count	≥1,000/mm3	442	87.7
	<1,000/mm3	60	11.9
	Not available	2	0.4

IQR: inter-quartile range, HIV: human immunodeficiency virus; TB: Tuberculosis; *Includes diabetes mellitus, gastrectomy, gastric ulcer, renal failure and gout (hyperuricemia).

doi:10.1371/journal.pone.0023806.t001

HLA-DRB1 and HLA-DQB1 alleles and IFN-γ responses

Since QFT-IT is based on T-cell response to MTB-specific antigenic peptides that are presented with MHC class II molecules, we investigated the role of HLA-DRB1 and -DQB1 alleles. Among seven most common HLA-DRB1 and -DQB1 alleles tested in the population [13], the allele frequencies of HLA-DRB1*0701 and DQB1*0201 in the test-negative group were significantly higher than that of the positive group ($P<0.0001$ and $P=0.001$, respectively, which remained significant after Bonferroni's correction) (table 3).

Nonrandom association between HLA-DRB1*0701 and DQB1*0202 was tested and HLA-DRB1*0701 was found to be in moderate linkage disequilibrium (LD) with HLA-DQB1*0201 allele ($D' = 0.608$ and $r^2 = 0.235$) (table not shown). The TBAg-Nil values of IFN-γ in the HLA-DRB1*0701-negative/DQB1*0201-positive group were not significantly lower than those in the both negative group (6.65 IU/ml [IQR, 2.85–10.00 (16.06)] vs 7.76 IU/ml [IQR, 2.58–10.00 (14.87)], $P=0.989$), whereas the IFN-γ values in the HLA-DRB1*0701-positive/DQB1*0201-negative group was significantly lower than those in the both negative group (2.30 IU/ml [IQR, 1.22–4.44] vs 7.76 IU/ml [IQR, 2.58–10.00 (14.87)], $P<0.001$) (table not shown).

TBAg-Nil values of all four patients with two HLA-DRB1*0701 alleles (homozygous for HLA-DRB1*0701) were below 0.35 IU/ml or the cutoff value; three negative, one indeterminate and none had positive results. In patients with one HLA-DRB1*0701 allele (heterozygous for HLA-DRB1*0701), proportions of negative, indeterminate and positive results were 9.4% (5/53), 7.6% (4/53) and 83.0% (44/53). In patients with no HLA-DRB1*0701 alleles (homozygous for non-HLA-DRB1*0701), the proportions were 3.6% (16/447), 2.2% (10/447) and 94.2% (421/447) respectively. Overall distribution of QFT-IT results was significantly different among HLA-DRB1*0701 genotypes ($P<0.0001$). The effect of two HLA-DRB1*0701 alleles on QFT-IT negativity was significant (3/4 vs 16/447, $P=0.0002$), whereas the effect of one HLA-DRB1*0701 allele on QFT-IT negativity was weaker than that of two HLA-DRB1*0701 alleles (5/53 vs 3/4, $P=0.007$) and did not reach significant levels (5/53 vs 16/447, $P=0.06$) when "no alleles" was regarded as a category for reference purposes.

Distribution of IFN-γ values may provide information about the mechanism by which false negative results are observed. We reviewed the relationship between IFN-γ values and HLA-DRB1*0701 genotypes (Figure 1). HLA-DRB1*0701 genotype significantly affected TB-Ag specific IFN-γ response (TBAg-Nil) ($P<0.001$); The IFN-γ values in patients with two HLA-DRB1*0701 alleles (homozygous for HLA-DRB1*0701) were significantly lower than those in patients with one HLA-DRB1*0701 allele (heterozygous for HLA-DRB1*0701) (0.15 IU/ml [IQR, 0.06–0.26] vs 1.91 IU/ml [IQR, 0.65–4.21], $P=0.008$). As a reference, the median of IFN-γ values in patients who did not bear any HLA-DRB1*0701 alleles was 7.59 IU/ml [IQR, 2.63–10.00 (14.92)].

No association was clinically observed between HLA-DRB1*0701-containing genotype and disease severity assessed by either cavity or infiltrate on CXR respectively (data not shown). QFT-IT test was performed again after two months of anti-TB treatment in 17 out of 19 HIV-negative patients with QFT-IT-negative results. All 7 patients who carried one or two HLA-DRB1*0701 alleles showed negative results again, whereas it remained negative only in 6 out of 10 patients without carrying the HLA allele, though this difference did not reach significant levels ($P=0.103$).

Analysis of 51 HLA-DR alleles registered on the ProPred database revealed that the average number of epitopes predicted in the overall amino acid sequences of ESAT-6 (95 amino acids),

Table 2. QFT-IT results and HIV status in smear-positive/culture-positive pulmonary TB patients.

	Positive		Negative		Indeterminate		p*
	n	% (95% CI)	n	% (95% CI)	n	% (95% CI)	
All (n = 504)	465	92.3 (89.6–94.4)	24	4.8 (3.1–7.0)	15	3.0 (1.7–4.9)	
HIV positive (n = 44)	27	61.4 (45.5–75.6)	5	11.4 (3.8–24.6)	12	27.3 (15.0–42.8)	<0.001
HIV negative (n = 459)	437	95.2 (92.8 97.0)	19	4.1 (2.5 6.4)	3	0.7 (0.1 1.9)	

QFT-IT: QuantiFERON-TB Gold In-Tube; HIV: human immunodeficiency virus; TB: Tuberculosis; CI: Confidence interval.
*Comparison was made between HIV-positive and HIV-negative groups.

doi:10.1371/journal.pone.0023806.t002

Table 3. Frequencies of HLA class II alleles and QFT-IT positive/negative results.

Allele name	Number of alleles (% [95%CI])			*P**
	Total	IGRA positive	IGRA-negative	
	2n‡ = 1008	2n = 930	2n = 48	
HLA-DRB1				
1202	337 (33.4 [30.5–36.4])	318 (34.2 [31.1–37.3])	11 (22.9 [12.0–37.3])	0.119
0901	129 (12.8 [10.8–15.0])	119 (12.8 [10.7–15.1])	6 (12.5 [4.7–25.2])	>0.999
0701	61 (6.1 [4.7–7.7])	44 (4.7 [3.5–6.3])	11 (22.9 [12.0–37.3])	<0.0001
1502	59 (5.9 [4.5–7.5])	53 (5.7 [4.3–7.4])	5 (10.4 [3.5–22.7])	0.198
0301	54 (5.4 [4.0–6.9])	49 (5.3 [3.9–6.9])	4 (8.3 [2.3–20.0])	0.324
0803	53 (5.3 [4.0–6.8])	51 (5.5 [4.1–7.1])	0 (0.0 [0.0–7.4])	0.170
1001	51 (5.1 [3.8–6.6])	49 (5.3 [3.9–6.9])	2 (4.2 [0.5–14.3])	>0.999
others	264 (26.2 [23.5–29.0])	247 (26.6 [23.7–29.5])	9 (18.8 [8.9–32.6])	0.312
HLA-DQB1				
0301	383 (38.0 [35.0–41.1])	361 (38.8 [35.7–42.0])	12 (25.0 [13.6–39.6])	0.067
0303	152 (15.1 [12.9–17.4])	138 (14.8 [12.6–17.3])	9 (18.8 [8.9–32.6])	0.414
0501	94 (9.3 [7.6–11.3])	87 (9.4 [7.6–11.4])	6 (12.5 [4.7–25.2])	0.448
0201	92 (9.1 [7.4–11.1])	74 (8.0 [6.3–9.9])	12 (25.0 [13.6–39.6])	0.001
0502	81 (8.0 [6.4–9.9])	76 (8.2 [6.5–10.1])	3 (6.3 [1.3–17.2])	>0.999
0601	70 (6.9 [5.5–8.7])	68 (7.3 [5.7–9.2])	0 (0.0 [0.0–7.4])	0.072
0401	42 (4.2 [3.0–5.6])	40 (4.3 [3.1–5.8])	1 (2.1 [0.1–11.1])	0.717
others	94 (9.3 [7.6–11.3])	86 (9.2 [7.5–11.3])	5 (10.4 [3.5–22.7])	0.797

*Comparison was made between QFT-IT-positive and -negative groups. After Bonferroni's correction, $P < 0.006$ was statistically significant, considering the number of comparisons.
‡Allele number is shown.
HLA: Human leukocyte antigen; QFT-IT: QuantiFERON-TB Gold In-Tube.
doi:10.1371/journal.pone.0023806.t003

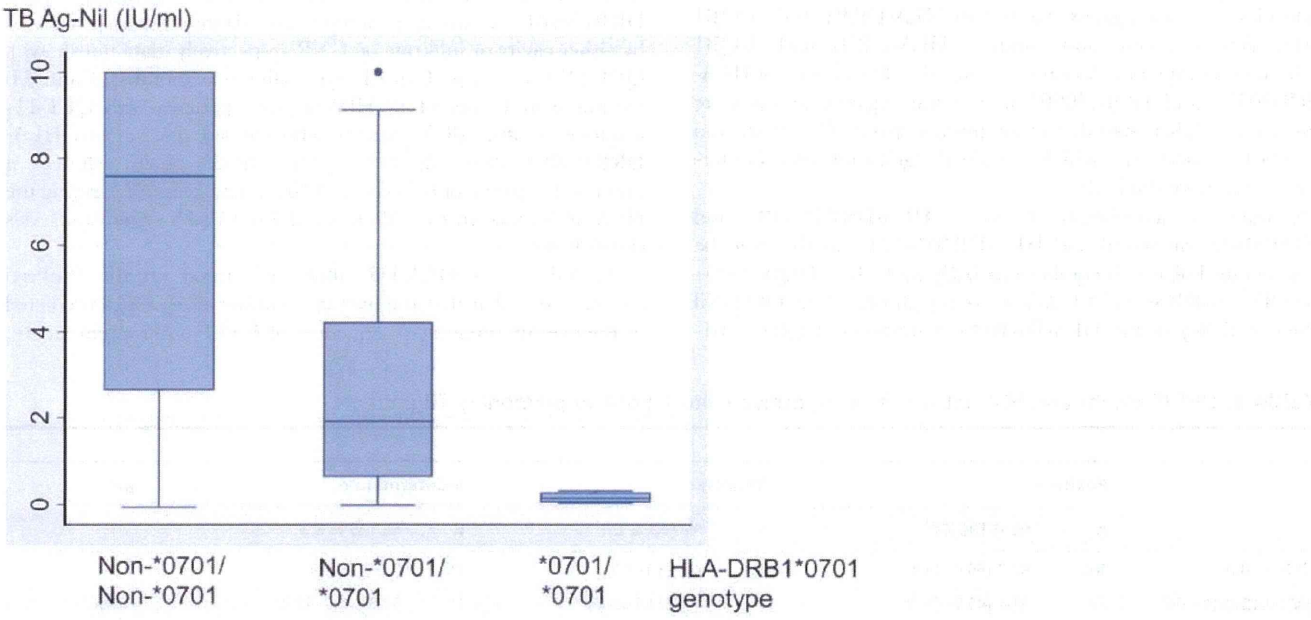

Figure 1. IFN-γ response to TB antigens stratified by HLA-DRB1*0701 genotypes in smear-positive/culture-positive pulmonary TB patients (n = 504). HLA-DRB1*0701 genotype significantly affected TB-Ag specific IFN-γ response (TBAg-Nil) ($P<0.001$). IFN: Interferon; TB: Tuberculosis; HLA: Human leukocyte antigen; Ag: Antigen.
doi:10.1371/journal.pone.0023806.g001

CFP10 (100 amino acids) and TB7.7 p4 (18 amino acids) to bind a given allele was median of 4 with IQR in 3 to 5, but the number of epitopes predicted for HLA-DRB1*0701 was only one (data not shown).

Univariate analysis

Host factors including age, sex, BMI, underlying diseases, disease status, and inherent characteristics of pathogen were analyzed. The number of HLA-DRB1*0701 alleles carried by the patients appeared to be associated with the test-negative results. For this reason, this variable was also included in the statistical model.

In univariate analysis, increased age by year, BMI<16.0, HIV co-infection and the number of HLA-DRB1*0701 alleles carried by patients showed significant associations with the negative results (OR = 1.04 [95%CI, 1.01–1.06], 7.27 [95%CI, 2.17–24.38], 4.26 [95%CI, 1.48–12.28], and 5.47 [95%CI, 2.58–11.61] respectively) (table 4). Sex, underlying diseases other than HIV infection, hospitalization, presence of infiltrates in more than half of the lung field and cavitary lesions on chest X-ray (CXR) did not show significant associations (data not shown). Beijing MTB strains were less frequently seen in the test-negative group (OR = 0.29 [95% CI, 0.11–0.76]). Multi-drug resistant (MDR)-TB strains showed no association with IGRA-negative results.

With QFT-IT indeterminate results, HIV co-infection, low lymphocyte count, MDR and the number of HLA-DRB1*0701 alleles showed significant associations (OR = 64.74 [95% CI, 17.23–243.20], 26.19 [95% CI, 8.00–85.72], 6.37 [95% CI, 1.64–24.68] and 4.66 [95% CI, 1.83–11.88], respectively).

Multivariate analysis

Age, sex, BMI, HIV status, lymphocyte count, and the number of HLA-DRB1*0701 alleles were put into the initial model for multivariate analysis. MTB strain and MDR-TB were not put together into this model because of the considerable number of missing values but analyzed separately as described later. In the final model, increased age by year, BMI <16.0, HIV co-infection and the number of HLA-DRB1*0701 alleles showed significant association with QFT-IT negativity (OR = 1.04 [95% CI, 1.01–1.07], 5.42 [95% CI, 1.48–19.79], 6.38 [95% CI, 1.78–22.92] and 5.09 [95% CI, 2.31–11.22] respectively) (table 5).

HIV co-infection and the number of HLA-DRB1*0701 alleles were also significantly associated with QFT-IT indeterminate results (OR = 99.59 [95% CI, 15.85–625.61] and 4.25 [95% CI, 1.27–14.16] respectively).

When non-positive (negative and indeterminate) results of QFT-IT were compared with positive results, increased age by year, BMI <16.0, HIV co-infection and the number of HLA-DRB1*0701 alleles showed similarly high odds ratios (Table S1).

Bacterial characteristics and IFN-γ responses

Among 488 patients for whom information of QFT-IT and MTB strains were both available, concentrations of IFN-γ responding to MTB-specific antigens were neither different between patient groups with Beijing and non-Beijing MTB strains (6.92 IU/ml [2.19–10.00 (14.42)] vs 6.00 IU/ml [2.12–10.00 (14.54)]) nor between patient groups with MDR-TB and non-MDR-TB strains (4.19 IU/ml [0.62–10.00 (15.72)] vs 6.57 IU/ml [2.19–10.00 (14.47)]) (table not shown).

Discussion

We calculated the test sensitivity of ELISA-based IGRA among active TB patients in Viet Nam and made an extensive analysis of the factors associated with the false-negative results, which include increased age by year, extremely low BMI, HIV co-infection, and the number of HLA-DRB1*0701 alleles carried by the patients.

Aging is known as a risk factor for false-negative results [19,20]. Kobashi et al. [19] reports that the positive rate for both ESAT-6 and CFP-10 antigens of QuantiFERON TB-2G tested in the patients ≥80 years old is significantly lower than that in younger patients. In another study conducted by Liao et al. [20], using ELISPOT assay, increasing age is associated with false-negative results. HIV co-infection was associated with indeterminate results as well as false-negative results, presumably due to strong suppression of mitogenic response [21].

Severe wasting disease or malnutrition causes unhealthy emaciation with extremely low BMI, debilitating the patients and also suppressing systemic immune response [22]. In our study, BMI <16.0 kg/m^2, was significantly associated with IGRA negativity whereas moderate and mild underweight (BMI from 16.0 to less than 18.5) were not. The proportion of BMI <18.5 in the general population in Hanoi was only 13.3% [23], indicating that very low BMI in our study population is associated with active TB disease. However, it is not known whether this emaciation is observed mainly as a result of the current wasting disease or partly a risk factor for disease development.

In this study, we newly demonstrated that a particular MHC class II allele, HLA-DRB1*0701, was strongly associated with low TBAg-Nil values observed in indeterminate and negative results. HLA-DRB1*0701-positive/DQB1*0201-negative group but not HLA-DRB1*0701-negative/DQB1*0201-positive group suppressed the IFN-γ response, which suggests that HLA-DQB1*0701, but not HLA-DQB1*0201 has a primary role. The negative effect of HLA-DRB1*0701 on the IFN-γ values appeared to intensify in proportion to the number of HLA-DRB1*0701 alleles. The association between the increased number of the HLA alleles and QFT-IT negative results was demonstrated by the analysis using a logistic regression model.

After two months of anti-TB treatment, all of our IGRA-negative patients bearing the HLA allele continued to show negative IGRA results. There was no significant association between the extent of disease on CXR and the HLA-DRB1*0701 genotype (data not shown), suggesting that the allele does not seem to affect the assay results through modulation of disease severity. *In silico* analysis suggested the low affinity of HLA-DRB1*0701 in binding with both ESAT-6 and CFP10 epitopes, and possibly failing to present them to T-cells for initiation of Th1 immune response efficiently [24].

Considering the low frequency of HLA-DRB1*0701 in the population tested, this finding may not have major clinical implications. However, we should bear in mind that negative QFT-IT results might be experienced in TB-infected individuals within a certain genetic background of the host even without apparent cause of immunodeficiency. In addition, it might be necessary to be investigated carefully in Southwestern Europe, North Africa, East Sub-Saharan Africa, West and South Asia among others, where high frequency (>15%) of the allele has been reported [25] and more than 2% of the people are supposed to possess this allele as homozygote. Further clinical investigations about HLA type and IGRA and *in vitro* experiments would contribute to a better understanding of IGRA performance in general and of QFT-IT in particular.

In analogy with negative results of tuberculin skin testing occasionally obtained in severe TB disease [26], IGRA-false-negative results may be caused by inefficient activation of antigen-specific CD4 T-cells [27], based on poorly-defined regulatory mechanism [28,29]. T-cell trafficking to the active TB sites or

Table 4. Univariate analysis using polytomous logistic regression model for factors associated with QFT-IT-negative and -indeterminate results (n = 503).

		QFT-IT-negative results			QFT-IT-indeterminate results		
		Proportion (%)	OR*	95% CI	Proportion (%)	OR*	95% CI
Sex	Male	21/398 (5.3)	1.00		13/398 (3.3)	1.00	
	Female	3/105 (2.9)	0.52	0.15–1.78	2/105 (1.9)	0.56	0.12–2.52
Age (years)			1.04	1.01 1.06		0.98	0.94 1.02
BMI	18.5–24.9	4/217 (1.8)	1.00		3/217 (1.4)	1.00	
	<16.0	9/77 (11.7)	7.27	2.17 24.38	3/77 (3.9)	3.23	0.64 16.40
	16.0–18.5	11/206 (5.3)	3.10	0.97–9.92	9/206 (4.4)	3.39	0.90–12.70
	≥25.0	0/3 (0.0)	NA	NA	0/3 (0.0)	NA	NA
Underlying condition	None	20/434 (4.6)	1.00		14/434 (3.2)	1.00	
	One	4/61 (6.6)	1.43	0.47–4.34	1/61 (1.6)	0.51	0.07–3.96
	More than one	0/8 (0.0)	NA	NA	0/8 (0.0)	NA	NA
HIV status	Negative	19/459 (4.1)	1.00		3/459 (0.7)	1.00	
	Positive	5/44 (11.4)	4.26	1.48–12.28	12/44 (27.3)	64.74	17.23–243.20
Lymphocyte count (cells/mm3)	≥1,000	19/441 (4.3)	1.00		4/441 (0.9)	1.00	
	<1,000	5/60 (8.3)	2.51	0.89–7.04	11/60 (18.3)	26.19	8.00–85.72
Direct smear result	Scanty	3/65 (4.6)	1.00		3/65 (4.6)	1.00	
	1+ and more	21/438 (4.8)	1.02	0.30–3.52	12/438 (2.7)	0.58	0.16–2.13
Cavity on CXR	No	6/145 (4.1)	1.00		9/145 (6.2)	1.00	
	Yes	16/327 (4.9)	1.13	0.43–2.95	4/327 (1.2)	0.19	0.06–0.62
Infiltrate in >3 lung zones	No	15/391 (3.8)	1.00		12/391 (3.1)	1.00	
	Yes	7/83 (8.4)	2.26	0.89–5.75	1/83 (1.2)	0.40	0.05–3.16
Hospitalization	No	17/375 (4.5)	1.00		9/375 (2.4)	1.00	
	To TB ward	5/104 (4.8)	1.10	0.40–3.07	6/104 (5.8)	2.50	0.87–7.21
	To ER	2/24 (8.3)	1.87	0.41–8.59	0/24 (0.0)	NA	NA
HLA-DRB1*0701 (the number of alleles)			5.47†	2.58–11.61		4.66†	1.83–11.88
MDR	No	21/466 (4.5)	1.00		12/466 (2.6)	1.00	
	Yes	2/22 (9.1)	2.43	0.53–11.19	3/22 (13.6)	6.37	1.64–24.68
MTB strain	Non-Beijing	17/229 (7.4)	1.00		8/229 (3.5)	1.00	
	Beijing	6/259 (2.3)	0.29	0.11–0.76	7/259 (2.7)	0.73	0.26–2.03

QFT-IT: QuantiFERON-TB Gold In-Tube; BMI: Body mass index; CXR: Chest X-ray; MDR: Multi drug resistance; TB: Tuberculosis; ER: Emergency room; MTB: *Mycobacterium tuberculosis;* CI: Confidence interval; NA: Not available.

*OR: Multinomial odds ratio, also known as relative risk ratio, that is obtained by exponentiating the logit coefficient.

†OR per unit change in the number of alleles: Distribution of QFT-IT results and the number of HLA-DRB1*0701 alleles was shown in the text.

doi:10.1371/journal.pone.0023806.t004

compartmentalization may also be involved in the suppressive response in circulating blood [28]. However, this mechanism may not explain a major part of false-negative results in our study because the extent of infiltrates or presence of cavity on CXR did not show significant effects on the assay results.

Beijing MTB strains have spread rapidly in Asia and previous reports show that these are more adapted to the human body evading immune mechanism than others [30]. Although an inverse association was apparently observed between isolation of Beijing strains and IGRA negativity in our study, it may be attributed to unknown factors we could not access, since we made no demonstration of difference in TBAg-induced IFN-γ levels between Beijing and non-Beijing strains.

The overall sensitivity of QFT-IT in our population was considerably high among high TB burden countries from Cape Town in South Africa, the Gambia, Zambia, India, and some other countries [3]. This seems to be due to the lower proportion of false-negative results in our study (4.8%) compared to (9.1% to 29%) in those studies. Several possible reasons for the interpretation of this point derive from our findings and others [19,20]: low proportion of underlying diseases including HIV, very few patients receiving immunosuppressive therapy, and recruitment of only new patients with sputum smear-confirmed pulmonary TB.

Our study had some limitations. Firstly, a clinical laboratory to measure CD4 count was not accessible during the study period, although CD4 count is an important parameter for this assessment [31]. Decrease in total lymphocyte count was used as a surrogate marker. Secondly, only smear-positive patients without previous treatment have been recruited, which may not allow us to generalize our results to all types of TB. Thirdly, further investigation is necessary to know whether all of the factors identified here affect results of ELISPOT-based IGRA as well. Lastly, the number of patients showing negative results was rather small despite the large number of recruited patients in our study.

Table 5. Multivariate analysis using polytomous logistic regression model for factors associated with QFT-IT-negative and -indeterminate results (n = 503).

		QFT-IT-negative results			QFT-IT-indeterminate results		
		Proportion (%)	OR*	95% CI	Proportion (%)	OR*	95% CI
Age (years)			1.04	1.01 1.07		1.04	0.97 1.11
BMI	18.5–24.9	4/217 (1.8)	1.00		3/217 (1.4)	1.00	
	<16.0	9/77 (11.7)	5.42	1.48 19.79	3/77 (3.9)	1.82	0.29 11.18
	16.0–18.5	11/206 (5.3)	2.65	0.79–8.85	9/206 (4.4)	1.92	0.43–8.48
	≥25.0	0/3 (0.0)	NA	NA	0/3 (0.0)	NA	NA
HIV status	Negative	19/459 (4.1)	1.00		3/459 (0.7)	1.00	
	Positive	5/44 (11.4)	6.38	1.78 22.92	12/44 (27.3)	99.59	15.85 625.61
HLA-DRB1*0701 (the number of alleles)			5.09†	2.31–11.22		4.25†	1.27–14.16

QFT-IT: QuantiFERON-TB Gold In-Tube; BMI: Body mass index; HIV: human immunodeficiency virus; CI: Confidence interval; NA: Not available.
*OR: Multinomial odds ratio, also known as relative risk ratio, that is obtained by exponentiating the logit coefficient.
†OR per unit change in the number of alleles: Distribution of QFT-IT results and the number of HLA-DRB1*0701 alleles was shown in the text.
doi:10.1371/journal.pone.0023806.t005

This is a limitation to analyze statistical significance in general. However, we were able to identify a novel host genetic factor, HLA*DRB1-0701. If well-known factors such as HIV co-infection were predominant in the studied population, individuals bearing the host genetic factor might have a chance of having those extrinsic factors together and it might be difficult to demonstrate that their genetic difference is a primary cause of false negativity.

Although some of the factors associated with IGRA-negative results have been proposed or even studied adopting a piecemeal method [2,3], the strong point of our study is that effects of all factors have been evaluated simultaneously by using appropriate statistical models, which provided a comprehensive insight into this area of interest.

In conclusion, we identified a specific HLA class II allele and characterized a variety of factors that possibly lead to false negativity of IGRA in active pulmonary TB. Detailed investigation of these unfavorable factors is necessary and would help to understand further the performance of the assay.

Supporting Information

Table S1 Univariate and multivariate analysis using logistic regression model for factors associated with QFT-IT non-positive (negative and indeterminate) results (n = 503).
(DOC)

Acknowledgments

The authors would like to thank Dr. Nguyen Phuong Hoang, Dr. Bui Thi Nguyet, Ms. Vu Thi Xuan Thu, Dr. Pham Tuan Phuong, Dr. Pham Thu Anh (Hanoi Lung Hospital), Dr. Tran Thi Bich Thuy (National Lung Hospital), Dr. Phan Thi Minh Ngoc, Ms. Nguyen Thi Ha (NCGM-BMH Medical Collaboration Center) and all healthcare staff of relevant district TB centers for supporting site implementation. The authors thank Dr. Masaki Matsushita (Wakunaga Pharmaceutical Co., Ltd) for technical support of HLA typing. The authors thank Kazuko Tanabe D.V.M. and Mr. John Crosskey for their critical reading of this manuscript.

Author Contributions

Conceived and designed the experiments: NTLH LTL N. Kobayashi SS PHT N. Keicho. Performed the experiments: NTLH LTL PHT LTH DBT MH IM NVH. Analyzed the data: NTLH TS N. Keicho. Contributed reagents/materials/analysis tools: KH NH N. Keicho. Wrote the paper: NTLH N. Keicho.

References

1. WHO Global Tuberculosis Control. Geneva: World Health Organization. Available: http://whqlibdoc.who.int/publications/2010/9789241564069_eng.pdf. Accessed 2011 July 27.
2. Pai M, Menzies D (2007) Interferon-à release assays: what is their role in the diagnosis of active tuberculosis? Clin Infect Dis 44: 74–77.
3. Dheda K, van Zyl Smit R, Badri M, Pai M (2009) T-cell interferon-γ release assays for the rapid immunodiagnosis of tuberculosis: clinical utility in high-burden vs. low-burden settings. Curr Opin Pulm Med 15: 188–200.
4. Diel R, Loddenkemper R, Nienhaus A (2010) Evidence-based comparison of commercial interferon-γ release assays for detecting active TB: a metaanalysis. Chest 137: 952–968.
5. European Centre for Disease Prevention and Control (2011) Use of interferon-gamma release assays in support of TB diagnosis. Stockholm: ECDC. Available: http://ecdc.europa.eu/en/publications/Publications/1103_GUI_IGRA.pdf. Accessed 2011 May 4.
6. Centers for Disease Control and Prevention (2010) Updated Guidelines for Using Interferon Gamma Release Assays to Detect *Mycobacterium tuberculosis* Infection — United States. MMWR 2010; 59. Available: http://www.cdc.gov/mmwr/pdf/rr/rr5905.pdf. Accessed 2011 March 31.
7. Sester M, Sotgiu G, Lange C, Giehl C, Girardi E, et al. (2011) Interferon-γ release assays for the diagnosis of active tuberculosis: a systematic review and meta-analysis. Eur Respir J 37: 100–111.
8. Ling DI, Pai M, Davids V, Brunet L, Lenders L, et al. (2011) Are interferon-{gamma} release assays useful for active tuberculosis in a high-burden setting? Eur Respir J. In press.
9. Mustafa AS, Oftung F, Amoudy HA, Madi NM, Abal AT, et al. (2000) Multiple epitopes from the *Mycobacterium tuberculosis* ESAT-6 antigen are recognized by antigen-specific human T cell lines. Clin Infect Dis 30: S201–205.
10. Brudey K, Driscoll JR, Rigouts L, Prodinger WM, Gori A, et al. (2006) *Mycobacterium tuberculosis* complex genetic diversity: mining the fourth international spoligotyping database (SpolDB4) for classification, population genetics and epidemiology. BMC Microbiol 6: 23.
11. Cellestis website. QuantiFERON®-TB Gold In-Tube. Available: http://www.cellestis.com/IRM/Content/usa/qftproducts_tbgoldintube.html. Accessed 2011 July 27.
12. Hang NT, Ishizuka N, Keicho N, Hong LT, Tam DB, et al. (2009) Quality assessment of an interferon-γ release assay for tuberculosis infection in a resource-limited setting. BMC Infect Dis 9: 66.

13. Hoa BK, Hang NT, Kashiwase K, Ohashi J, Lien LT, et al. (2008) HLA-A, -B, -C, -DRB1 and -DQB1 alleles and haplotypes in the Kinh population in Vietnam. Tissue Antigens 71: 127–134.
14. Broad Institute website. Haploview. Available: http://www.broadinstitute.org/scientific-community/science/programs/medical-and-population-genetics/haploview/haploview. Accessed 2011 July 27.
15. Barrett JC, Fry B, Maller J, Daly MJ (2005) Haploview: analysis and visualization of LD and haplotype maps. Bioinformatics 21: 263–265.
16. Bioinformatics Center IMTECH website. Propred. MHC Class-II Binding Peptide Prediction Server. Available: http://www.imtech.res.in/raghava/propred. Accessed 2011 July 27.
17. Singh H, Raghava GP (2001) ProPred: prediction of HLA-DR binding sites. Bioinformatics 17: 1236–1237.
18. WHO Expert Consultation (2004) Appropriate body-mass index for Asian populations and its implications for policy and intervention strategies. Lancet 363: 157–163.
19. Kobashi Y, Mouri K, Yagi S, Obase Y, Miyashita N, Okimoto N, et al. (2008) Clinical utility of the QuantiFERON TB-2G test for elderly patients with active tuberculosis. Chest 133: 1196–1202.
20. Liao CH, Lai CC, Tan CK, Chou CH, Hsu HL, Tasi TH, et al. (2009) False-negative results by enzyme-linked immunospot assay for interferon-gamma among patients with culture-confirmed tuberculosis. J Infect 59: 421–423.
21. Syed Ahamed Kabeer B, Sikhamani R, Swaminathan S, Perumal V, Paramasivam P, et al. (2009) Role of interferon γ release assay in active TB diagnosis among HIV infected individuals. PLoS One 4: e5718.
22. Schluger NW, Rom WN (1998) The host immune response to tuberculosis. Am J Respir Crit Care Med 157: 679–691.
23. Walls HL, Peeters A, Son PT, Quang NN, Hoai NT, Loi do D, et al. (2009) Prevalence of underweight, overweight and obesity in urban Hanoi, Vietnam. Asia Pac J Clin Nutr 18: 234–239.
24. Arend SM, Geluk A, van Meijgaarden KE, van Dissel JT, Theisen M, et al. (2000) Antigenic equivalence of human T-cell responses to *Mycobacterium tuberculosis*-specific RD1-encoded protein antigens ESAT-6 and culture filtrate protein 10 and to mixtures of synthetic peptides. Infect Immun 68: 3314–3321.
25. dbMHC IHWG Projects website. Anthropology. Class II Allele Frequencies. Available: http://www.ncbi.nlm.nih.gov/projects/gv/mhc/ihwg.cgi?cmd=pagv&page=AnthroMain. Accessed 2011 July 27.
26. Diagnostic Standards and Classification of Tuberculosis in Adults and Children (2000) Am J Respir Crit Care Med 161: 1376–1395.
27. Pathan AA, Wilkinson KA, Klenerman P, McShane H, Davidson RN, et al. (2001) Direct ex vivo analysis of antigen-specific IFN-ã-secreting CD4 T cells in *Mycobacterium tuberculosis*-infected individuals: associations with clinical disease state and effect of treatment. J Immunol 167: 5217–5225.
28. Jo EK, Park JK, Dockrell HM (2003) Dynamics of cytokine generation in patients with active pulmonary tuberculosis. Curr Opin Infect Dis 16: 205–210.
29. Dheda K, Schwander SK, Zhu B, van Zyl-Smit RN, Zhang Y (2010) The immunology of tuberculosis: from bench to bedside. Respirology 15: 433–450.
30. Parwati I, van Crevel R, van Soolingen D (2010) Possible underlying mechanisms for successful emergence of the *Mycobacterium tuberculosis* Beijing genotype strains. Lancet Infect Dis 10: 103–111.
31. Lugos MD, Adetifa IM, Donkor S, Hill PC, Adegbola RA, et al. (2009) Evaluation of the contribution of major T cell subsets to IFN-gamma production in TB infection by ELISPOT. Immunol Invest 38: 341–349.

J Occup Health 2011; 53: 234–239

Journal of Occupational Health

Brief Report

Pulmonary Toxicity in Mice by 2- and 13-week Inhalation Exposures to Indium-tin Oxide and Indium Oxide Aerosols

Kasuke NAGANO[1], Tomoshi NISHIZAWA[1], Yoko EITAKI[2], Makoto OHNISHI[1], Tadashi NOGUCHI[1], Heihachiro ARITO[1] and Shoji FUKUSHIMA[1]

[1]Japan Bioassay Research Center, Japan Industrial Safety and Health Association and [2]Occupational Health Research and Development Center, Japan Industrial Safety and Health Association, Japan

Abstract: Pulmonary Toxicity in Mice by 2- and 13-week Inhalation Exposures to Indium-tin Oxide and Indium Oxide Aerosols: Kasuke NAGANO, *et al.*, Japan Bioassay Research Center, Japan Industrial Safety and Health Association—Objectives: Inhalation toxicities of indium-tin oxide (ITO) and indium oxide (IO) in mice were characterized in comparison with those previously reported in rats. **Methods:** B6C3F$_1$ mice of both sexes were exposed by inhalation to ITO or IO aerosol for 6 h/day, 5 day/wk for 2 wk at 0, 0.1, 1, 10 or 100 mg/m^3 or 13 wk at 0, 0.1or 1 mg/m^3. **Results:** ITO and IO particles were deposited in the lung, mediastinal lymph node (MLN) and nasal-associated lymphoid tissue. Alveolar proteinosis, infiltrations of alveolar macrophages and inflammatory cells and increased lung weight were induced by 2- and 13-week exposures to ITO and IO, while alveolar epithelial hyperplasia occurred only in the 2-week exposures. Thickened pleural wall, hyperplastic MLN, extramedullary hematopoiesis in the spleen and increased levels of erythrocyte parameters were induced by 13-week exposure to ITO. The ITO- and IO-induced pulmonary lesions were milder in mice than those previously reported in rats, and the fibrotic lesions were different between these two species. Indium levels in the lung and pooled blood were analyzed in the mice exposed to ITO and IO for 13 wk. In the 13-week inhalation exposure of mice to ITO, alveolar proteinosis and significantly increased lung weight were induced at the same exposure concentration as the current threshold limit value for indium and its compounds.
(J Occup Health 2011; 53: 234–239)

Received Dec 2, 2010; Accepted Jan 25, 2011
Published online in J-STAGE Mar 16, 2011
Correspondence to: T. Nishizawa, Japan Bioassay Research Center, Japan Industrial Safety and Health Association, 2445 Hirasawa, Hadano, Kanagawa 257-0015, Japan
(e-mail: t-nishizawa@jisha.or.jp)

Key words: Indium oxide, Indium-tin oxide, Inhalation, Lung, Mouse, Toxicity

Serious concerns have been raised over workers' health in the plants where indium-tin oxide (ITO) is manufactured and processed. Fatal case studies[1, 2] and epidemiology studies of workers[3–6] have demonstrated that inhalation of indium is a potential cause of occupational lung disease and increases the risk of interstitial lung damage. Experimental toxicology studies have shown that an intratracheal administration of ITO powder induces persistent inflammation in the lung without any significant fibrotic response in rats[7], and elicits pulmonary inflammatory response with diffuse alveolar or bronchiolar cell hyperplasia and interstitial fibrotic proliferation in hamsters[8, 9]. Our previous study[10] showed that 2- and 13-week inhalation exposures of rats to ITO or indium oxide (IO) aerosol induce pulmonary fibrosis, alveolar proteinosis and macrophage infiltration.

The present studies were intended to characterize inhalation toxicities of ITO and IO aerosols in mice in comparison with those reported in rats[10].

Materials and Methods

The present studies were performed with the approval of the ethics committee of the Japan Bioassay Research Center. The animals were cared for in accordance with a guide for the care and use of laboratory animals. All these related documentations were cited in our previous rat studies[10].

ITO and IO powders were the same as those used in our previous rat studies[10], which were kindly supplied by JX Nippon Mining & Metals, Corp (Tokyo, Japan).

B6C3F$_1$/Crlj mice of both sexes were obtained at the age of 4 wk from Charles River Japan, Inc (Kanagawa, Japan). The animals were quarantined and acclimated for 2 wk before the start of experiment. The mice were individually housed in stainless-steel wire hanging cages